

DETC2008-49538

PRECISION CIRCULAR WALKING OF BIPEDAL ROBOTS

Karl J. Muecke

Robotics and Mechanisms Laboratory
Dept. of Mechanical Engineering
Virginia Tech
Blacksburg, Virginia 24060
Email: kmuecke@vt.edu

Dennis W. Hong

Robotics and Mechanisms Laboratory
Dept. of Mechanical Engineering
Virginia Tech
Blacksburg, Virginia 24060
Email: dhong@vt.edu

Seungchul Lim

Dept. of Mechanical Engineering
MyongJi University
Yongin, KOREA, 449-728
Email: slim@mju.ac.kr

ABSTRACT

Whenever bipedal robots need to make turns, the ability to walk stably and precisely along a circular curve of an arbitrary radius will be quite beneficial. This motivates us to derive new Zero Moment Point (ZMP) constraint equations with respect to a rotating coordinate frame, seek appropriate dynamic gaits based on them, and address the forward and inverse kinematics. After the relevant body and feet trajectories are fully prescribed, joint motions are determined using the inverse kinematics. A set of dynamic walking patterns including the transient are herein proposed and applied to an exemplificative case of turning locomotion. Conclusively, dynamic simulations prove the patterns to be successful even in the presence of distributed-mass and ground contact effects.

INTRODUCTION

In order to be a successful and anthropomorphic bipedal robot, it needs to be able to turn. The ability to walk stably and precisely along a circular curve of an arbitrary radius will be quite beneficial for such robots. Most paths, including straight lines, can be regarded as a continuation of circular curves of assorted sizes. Additionally, without accurate inverse kinematics, the robot may not be stable on such routes. This motivates us to derive new ZMP [1, 2] constraint equations with respect to a rotating coordinate frame, seek appropriate dynamic body motions based on them, and address the forward and inverse kinematics. It is generally accepted that robots must satisfy the ZMP con-

straint to be stable in motion; the ZMP is inside the stable region defined by the convex hull formed by the contact points between the feet and ground [2]. Making use of the rotating coordinate frame and inverse kinematics will help identify the centrifugal effect and prevent the body from tipping. Unfortunately, many robots are making turns that depend on poor joint kinematics, which come from either a teach-and-playback approach or a simply modified straight-walking pattern with pelvic yaws. This can lead to instability and the robots' body tipping. In this respect, an existing work [3] is noteworthy, but lacks important details such as inverse kinematics.

In here, a biped robot [1] with a typical 12 DOF lower body is selected as a sample, and the inverted pendulum model [2] is adopted to approximate its dynamic characteristics. The derived ZMP differential equation is highly nonlinear. So we take a reverse approach rather than directly solve the equation. In other words, we substitute the body motions, which are basically similar to straight walking patterns, into the ZMP equation to see how the ZMP moves. In addition to such a steady pattern, a transient walking pattern is also suggested to create smooth transitions between distinct gaits. After the relevant body and feet trajectories are fully prescribed in 3-D space, joint motions become available analytically due to the inverse kinematics herein disclosed. Finally the proposed set of dynamic walking patterns are applied to an exemplificative case of turning locomotion and proved successful by a dynamics analysis software, ADAMS [4], even in the presence of distributed-mass and ground contact effects.

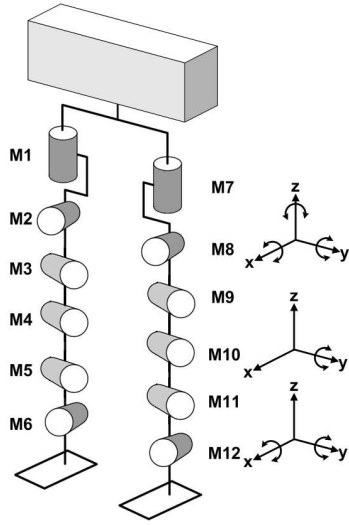


Figure 1. MECHANICAL STRUCTURE OF THE SAMPLE ROBOT.

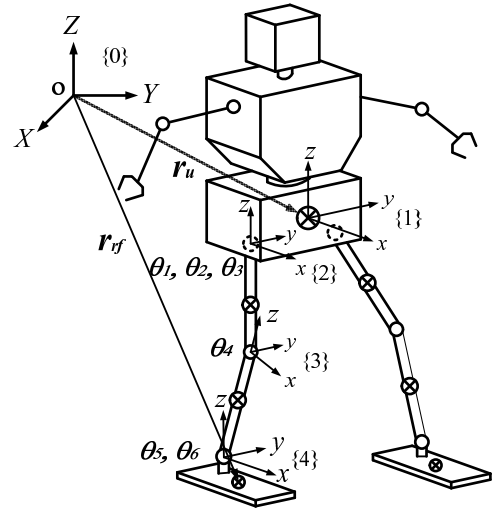


Figure 2. COORDINATE FRAMES IN USE.

SAMPLE ROBOT AND INVERSE KINEMATICS

As sketched in Fig. 1, the selected sample robot consists of a simple upper body and two symmetric legs with 6 DOFs each. The three axes at the pelvis and the two axes at ankle are modeled to intersect orthogonally at a single point (one point in the pelvis and one point in the ankle). Moreover each rotational axis is arranged in the sequence of yaw (M1/M7), roll (M2/M8), pitch (M3/M9), pitch (M4/M10), pitch (M5/M11), and roll (M6/M12) from top to bottom.

In order to address the kinematics, a series of coordinate frames are defined in Fig. 2; $\{0\}$ is the Cartesian inertial coordinate frame and all the others are link-fixed coordinate frames initially coincident with $\{0\}$ in directions. The position vector of the right foot from the body, $\mathbf{r}_{rf/u} (= \mathbf{r}_{rf} - \mathbf{r}_u)$, can be represented as below in terms of $\{1\}$, the body-fixed frame.

$${}^1\mathbf{r}_{rf/u} = {}^1\mathbf{x}_u + {}_2R^2\mathbf{x}_{rt} + {}_3R^3\mathbf{x}_{rs} + {}_4R^4\mathbf{x}_{rf}, \quad (1)$$

where ${}^1\mathbf{r}_{rf/u} = [x \ y \ z]^T$, ${}^1\mathbf{x}_u = [a_1 \ a_2 \ a_3]^T$, ${}^2\mathbf{x}_{rt} = [l_{tx} \ l_{ty} \ l_{tz}]^T$, ${}^3\mathbf{x}_{rs} = [l_{sx} \ l_{sy} \ l_{sz}]^T$, and ${}^4\mathbf{x}_{rf} = [l_{fx} \ l_{fy} \ l_{fz}]^T$. In fact, all the remaining magnitude values in Eqn. (1) are zeros except for $a_i (i = 1, 2, 3)$, l_{tz} , l_{sz} , l_{fx} , l_{fz} that respectively denote sizes of the upper body, thigh, shin, and foot. Now, introducing abbreviations such as $s_i = \sin\theta_i$, $c_i = \cos\theta_i$, $s_{ij} = \sin(\theta_i + \theta_j)$, $c_{ij} = \cos(\theta_i + \theta_j)$, etc, the detailed expressions for rotational matrices in Eqn. (1) are in the appendix as Eqn. (A10).

Suppose that the desired relative position and orientation between the body and the foot are respectively $[x \ y \ z]^T$ and α about the vertical axis for circular walking. Then, Eqns. (1) and (A10) can be combined and solved for corresponding joint angles, i.e.,

inverse kinematics solutions disclosed in the Appendix. From those, we can see that all of the joint angles must be functions of α , the body's yaw, to keep the body level. This assertion may be ignored only when robot turns in place or walks with a sufficiently small turning angle.

ZMP CONSTRAINTS AND PATTERN DESIGN

In this paper, a circular walking is studied with the trunk nominally upright and at the same height. Additionally, the supportive foot will be placed on the ZMP location tangentially to the circular path. During such a steady state turning, robots have a periodic motion. However, since robots tend to change gaits from one to another, some transient means is also needed to smooth transitions between different gaits. This aspect prompts us to devise both kinds of walking patterns. It is generally accepted that robots must satisfy the ZMP constraint to be stable in motion and the constraint itself may take a different form for different situations [2, 5, 6]. Figure 3 portrays yet another situation in which the robot is walking along a circle of radius r whose center is o' away from the reference point o by vector \mathbf{d} .

The position vector from point o to the center of mass G can be expressed as in Eqn. (2a) in terms of $\{C\}$, the cylindrical rotating coordinate frame. Likewise, its associated acceleration vector is obtainable through time-differentiation as in Eqn. (2b).

$$\mathbf{r}_u = \mathbf{d} + r\mathbf{e}_r + z\mathbf{k} \quad (2a)$$

$$\mathbf{a}_u = (\ddot{r} - r\dot{\theta}^2)\mathbf{e}_r + (2\dot{r}\dot{\theta} + r\ddot{\theta})\mathbf{e}_\theta + \ddot{z}\mathbf{k} \quad (2b)$$

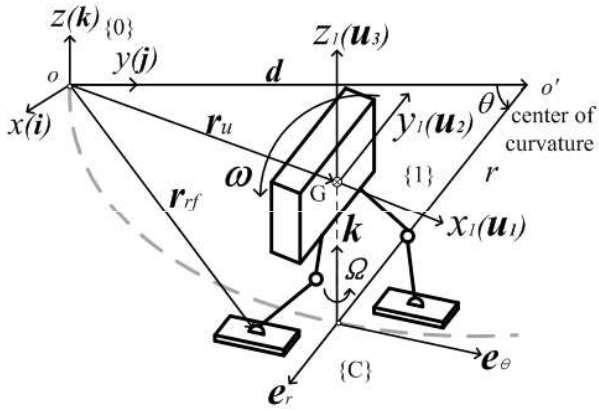


Figure 3. THE ROBOT IN CIRCULAR WALKING.

Next, assuming frame $\{1\}$ serves as the principal inertial axes and rotates only in the yaw direction at the angular acceleration $\ddot{\theta}$, the inertial forces and moments can be expressed in terms of $\{1\}$ that is just 90° rotated from $\{C\}$ excluding yaw angle. Written in Eqn. (3) are the forces and moments, where I_z denotes the body mass moment of inertia along the yaw direction.

$$\mathbf{F}_b = -m(2\dot{r}\dot{\theta} + r\ddot{\theta})\mathbf{u}_1 - m(-\ddot{r} + r\dot{\theta}^2)\mathbf{u}_2 - m\ddot{z}\mathbf{u}_3 \quad (3a)$$

$$\mathbf{M}_b = -I_z\ddot{\theta}\mathbf{u}_3 \quad (3b)$$

Finally, applying the force equilibrium condition to the robot, more specifically the point named the ZMP, gives the desired ZMP constraint equation. The derived equation can be found as Eqn. (4), in which the parameter $a (= \sqrt{g/z_b})$ remains constant unless the robot height, z_b , changes during walking. Figure 4 shows that all the inertial forces and moments including the centrifugal force are taken into account along with gravity. Henceforth, subscript b is attached to body-related variables like r_b and θ_b .

$$x_{ZMP} = -\frac{(2\dot{r}_b\dot{\theta}_b + r_b\ddot{\theta}_b)}{a^2}, y_{ZMP} = \frac{(\ddot{r}_b + r_b\dot{\theta}_b^2)}{a^2} \quad (4)$$

Unlike the case of straight walking, the ZMP equation in Eqn. (4) is a highly nonlinear, 4-th order differential equation, which is hard to solve for body motions given ZMP positions. So, we take a reverse approach by substituting some assumed body motions into the ZMP equation and see how the ZMP

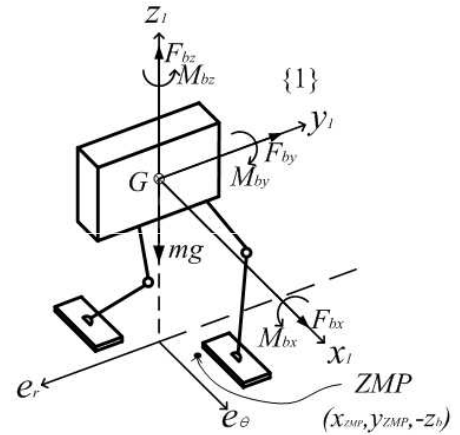


Figure 4. FORCES AND MOMENTS ACTING ON THE ROBOT.

moves. The motions are basically hyperbolic patterns [1, 5]—similar to straight walking patterns for more natural and stable turning. Therefore as depicted in Fig. 5, either zero or non-zero acceleration is imposed depending on how the robot is supported (namely, Double or Single Support Phase). The body motion is detailed in Eqns. (5,6).

$$r_b(\tau) = \begin{cases} (r_0 - r_{ZMP})\cosh a\tau + \frac{\dot{r}_0}{a}\sinh a\tau + r_{ZMP} & \text{for SSP} \\ -\dot{r}_0\tau + r_0 & \text{for DSP} \end{cases} \quad (5)$$

$$\theta_b(\tau) = \begin{cases} (\theta_0 - \theta_{ZMP1})\cosh a\tau + \frac{\dot{\theta}_{bD}}{a}\sinh a\tau + \theta_{ZMP1} & \text{for I} \\ \dot{\theta}_{bS}\tau + \theta_{ZMP1} & \text{for II} \\ \frac{\dot{\theta}_{bS}}{a}\sinh a\tau + \theta_{ZMP2} & \text{for III} \\ \dot{\theta}_{bD}\tau + \theta_{ZMP1} + \theta_{ZMP2} & \text{for IV} \end{cases} \quad (6)$$

By applying the motion continuity condition up to speed across each interval, one can get the same simultaneous algebraic equations as in [1]. The equations enable us to determine an adequate time duration of each interval for specified walking parameters such as r_{ZMP} , θ_{ZMP1} , θ_{ZMP2} , etc.

The ZMP location can be obtained in terms of $\{0\}$ as in Eqn. (7) via the coordinate transformation of its counterpart computed from Eqns. (4-6). Equation (8) shows the foot center location in $\{0\}$ as a function of the aforementioned input parameters.

$$\begin{pmatrix} X_{ZMP} \\ Y_{ZMP} \end{pmatrix} = \begin{pmatrix} (r_b - y_{ZMP})s\theta_b + x_{ZMP}c\theta_b \\ r_m + (y_{ZMP} - r_b)c\theta_b + x_{ZMP}s\theta_b \end{pmatrix} \quad (7)$$

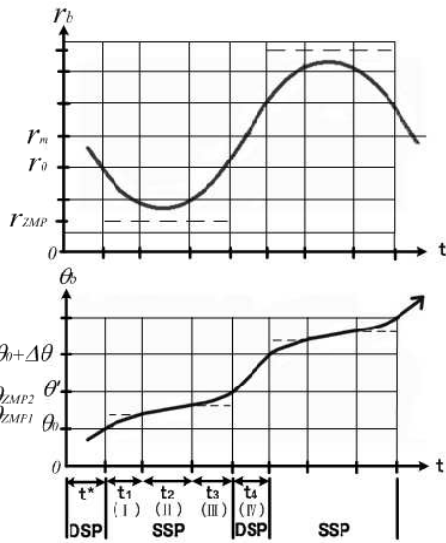


Figure 5. HYPERBOLIC STEADY WALKING PATTERN.

$$X_C = r_{ZMP} \bar{\theta}, Y_C = r_m - r_{ZMP} \bar{\theta} \quad (8)$$

where $\bar{\theta}$ is equal to $k\Delta\theta$, for the k -th footstep. Finally, as the transitional pattern connecting the initial stationary stance with the foregoing steady gaits, a cubic polynomial is suggested for each direction as in Eqn. (9). The coefficients depend on the position and speed at the initial (when $\tau=0$) and final (when $\tau=t^*$) moments of the transition—both of which are preferably DSP states for a larger stability margin.

$$r_b(\tau) = a_3\tau^3 + a_2\tau^2 + a_1\tau + a_0 \quad (9a)$$

$$\theta_b(\tau) = b_3\tau^3 + b_2\tau^2 + b_1\tau + b_0 \quad (9b)$$

DYNAMIC SIMULATIONS

The sample robot is 478mm high and 22.4kg heavy with about 80% of its weight in the upper body (Refer to Table 1). As before [1], the vertical reaction arising from ground contact is modeled to be the sum of nonlinear stiffness and viscous damping forces. Additionally, the thrust Coulomb friction force has the static and kinetic friction coefficients of 0.8 and 0.7 respectively.

Table 1. ROBOT SPECIFICATIONS

Part	Size(mm)	Mass(kg)
Body	196(W)x150(H)x60(T)	17.81
Right Leg	325(L)	2.150
Left Leg	325(L)	2.150
Right Foot	50(W)x110(L)x3(T)	0.1546
Left Foot	50(W)x110(L)x3(T)	0.1546
Total	-	22.42

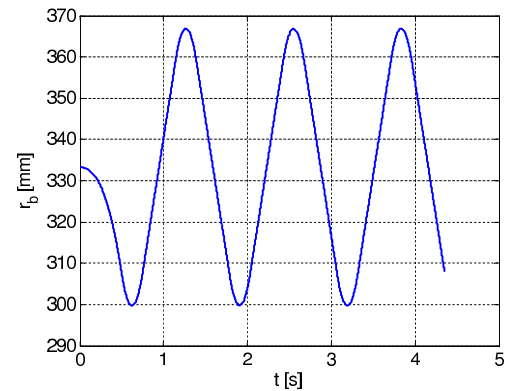


Figure 6. RADIAL BODY POSITION.

The following walking parameters were used: $z_b = 350mm$, $r_m = 333mm$, $r_{ZMP} = 68mm$, $\theta_0 = 0$, $\Delta\theta = 2\pi/30rad$, $\theta_{ZMP1} = \Delta\theta/8$, $\theta_{ZMP2} = \Delta\theta/4$, $\dot{\theta}_{bD} = 1.6 \Delta\theta rad/s$, $t^*=0.5s$. With this case, the aforementioned relevant equations [1] yield these outcomes: $t_1=t_3=0.0831s$, $t_2=0.0858s$, and $t_4=0.3906s$; making the period of steady walking 0.6426s long. For the entire time span of 4.35s, the robot takes 6 steps forward counting in the first transient step. The associated radial and tangential trajectories are plotted vs. time in Figs. 6 and 7; the corresponding body trajectory in terms of $\{0\}$ is shown in Fig. 8.

The foot motion is planned in 3-D space smoothly as shown in Figs. 9,10, and 11 where the first two are concerned with the horizontal direction and the last with the vertical direction. R and L denote the right and left foot respectively. As a result, the ZMP trajectory continues to stay well inside the stable regions formed by footprints throughout the walking (refer to Fig. 12).

The subsequent three figures demonstrate the dynamic simulation results using ADAMS. Figure 13 contains the successive snapshots of an animated motion captured every 0.5s from the start. It confirms that the robot walks precisely along the circular curve at an average speed of 112mm/s and turns at a rate of $12^\circ/step$ during steady state. As evidenced in Fig. 7, the body continuously faces the tangential direction of the circular

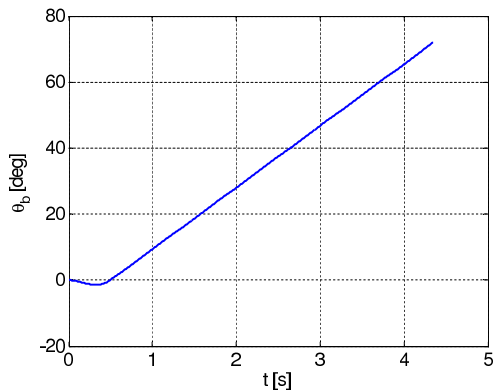


Figure 7. TANGENTIAL BODY POSITION.

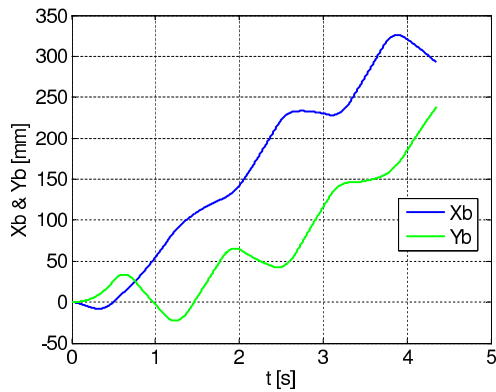


Figure 8. BODY POSITION IN FRAME $\{0\}$.

path. Fig. 14 shows the corresponding trajectories of the joint angles within the right leg along with their ranges and periodicity. Compared to Fig. 8 with only negligible errors, Fig. 15 once again verifies that a stable walking motion has been realized as planned.

CONCLUSIONS

In this paper, a new ZMP formula and the inverse kinematics solutions are derived for a precision circular walking pattern for biped robots. Based on the new formula and solutions, a dynamic steady walking pattern is suggested along with a transient transition between distinct gaits. Finally, such a set of dynamic walking patterns are applied to an exemplificative case of turning locomotion, where a biped robot with a typical structure walks along a circular path. The walking pattern is proved successful by dynamic simulations.

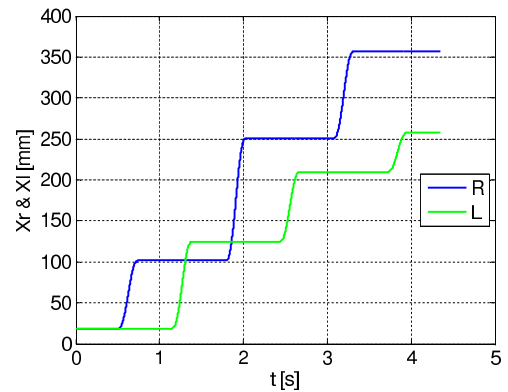


Figure 9. FOOT TRAJECTORY ALONG X-AXIS OF FRAME $\{0\}$.

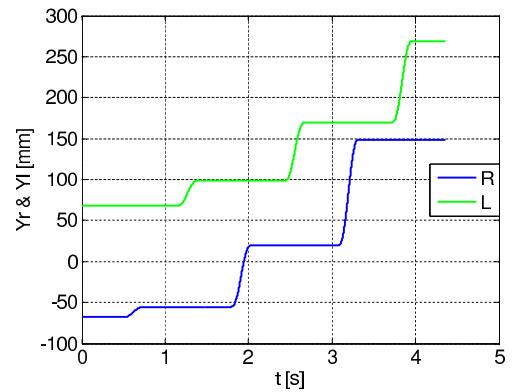


Figure 10. FOOT TRAJECTORY ALONG Y-AXIS OF FRAME $\{0\}$.

ACKNOWLEDGMENT

The authors would like to thank the Korea Science and Engineering Foundation (Grant No. KOSEF-R-01-2003-000-10014-0) and the National Science Foundation (Grant No. 0730206) for their support for this work.

REFERENCES

- [1] Lim, S., KIM, K., Son, Y., and Kang, H., 2005. "Walk simulations of a biped robot". *International Conference on Control, Automation, and Systems*.
- [2] Vukobratovic, M., Borovac, B., Surla, D., and Stokic, D., 1990. *Scientific Fundamentals of Robotics 7: Biped Locomotion*. Springer-Verlag.
- [3] Kajita, S., Kanehiro, F., Kaneko, K., Fujiwara, K., Yokoi, K., and Hirukawa, H., 2003. "Biped walking pattern generation by a simple three-dimensional inverted pendulum model". *Advanced Robotics*, **17**(2).
- [4] Inc, M. D., 2001. *Basic ADAMS Full Simulation Training Guide*.

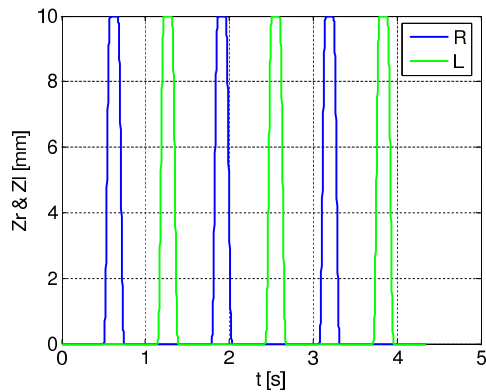


Figure 11. FOOT TRAJECTORY ALONG Z-AXIS OF FRAME $\{0\}$.

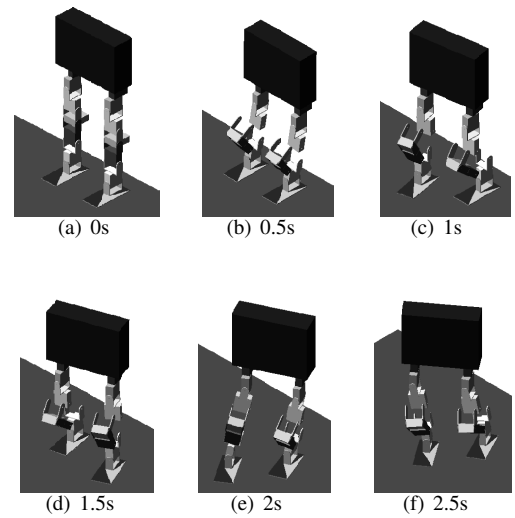


Figure 13. SNAPSHOTS OF THE ROBOT IN CIRCULAR WALKING

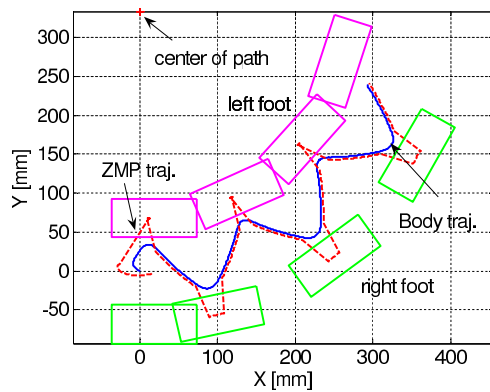


Figure 12. TRAJECTORIES OF THE BODY AND ZMP ON XY PLANE.

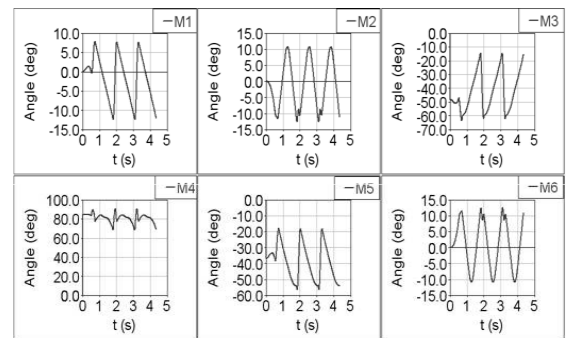


Figure 14. ANGLES OF JOINTS WITHIN THE RIGHT LEG.

Appendix A: Inverse Kinematic Solutions

$${}^1_2R = \begin{bmatrix} -s_1s_2s_3 + c_1c_3 & -s_1c_2 & s_1s_2c_3 + c_1s_3 \\ c_1s_2s_3 + s_1c_3 & c_1c_2 & -c_1s_2c_3 + s_1s_3 \\ -c_2s_3 & s_2 & c_2c_3 \end{bmatrix} \quad (10a)$$

$${}^1_3R = \begin{bmatrix} -s_1s_2s_3c_4 + c_1c_3c_4 & -s_1c_2 & s_1s_2c_3c_4 + c_1s_3c_4 \\ c_1s_2s_3c_4 + s_1c_3c_4 & c_1c_2 & -c_1s_2c_3c_4 + s_1s_3c_4 \\ -c_2s_3c_4 & s_2 & c_2c_3c_4 \end{bmatrix} \quad (10b)$$

$${}^1_4R = \begin{bmatrix} -s_1s_2s_3s_4c_5 + c_1c_3s_4c_5 & s_1s_2s_6c_3s_4c_5 + s_6c_1s_3s_4c_5 - s_1c_2c_6 \\ c_1s_2s_3s_4c_5 + s_1c_3s_4c_5 & -c_1s_2s_6c_3s_4c_5 + s_1s_6s_3s_4c_5 + c_1c_2c_6 \\ -c_2s_3s_4c_5 & s_6c_2c_3s_4c_5 + s_2c_6 \\ s_1s_2s_6c_3c_4s_5 + c_1c_6s_3c_4s_5 + s_1c_2s_6 \\ -c_1s_2c_6c_3c_4s_5 + s_1c_6s_3c_4s_5 - c_1c_2s_6 \\ c_2c_6c_3c_4s_5 - s_2s_6 \end{bmatrix} \quad (10c)$$

- [5] Lim, S., and Ko, I., 2006. "Locomotions of a biped robot: Static vs. dynamic gaits". *Journal of KSME*, **30**(6).
- [6] Lim, S., 2007. "Dynamic stair walking of biped humanoid robots". *Journal of Mechanical Science and Technology*, **21**(6).

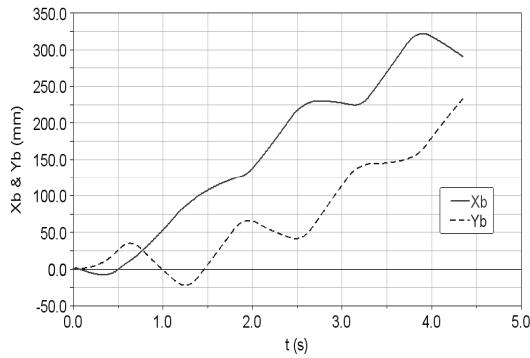


Figure 15. TORSO MOTIONS UNDER DYNAMIC EFFECTS.

$$q = l_{sz}^2(c_4^2 - 1) \{-2l_{tz}l_{sz}c_4 + (x - a_1)^2c^2\alpha - l_{sz}^2 - (y - a_2)^2c^2\alpha + (y - a_2)^2 - l_{tz}^2 + xys2\alpha - xa_2s2\alpha - 2l_{fx}ys\alpha - 2ya_1s2\alpha + l_{fx}^2 - 2xl_{fx}c\alpha + a_1a_2s2\alpha + 2l_{fx}a_2s\alpha + 2l_{fx}a_1c\alpha\}, \quad (16)$$

$$s_4 = \sqrt{1 - c_4^2} \quad (17)$$

$$c_4 = \{(x - a_1 - l_{fx}c\alpha)^2 + (y - a_2 - l_{fx}s\alpha)^2 + (z - a_3 - l_{fz})^2 - l_{sz}^2 - l_{tz}^2\} / (2l_{sz}l_{tz}). \quad (18)$$

$$\theta_1 = \alpha \quad (11a)$$

$$\theta_2 = -\sin^{-1}(v/\sqrt{w}) \quad (11b)$$

$$\theta_3 = \text{Atan2}(s_3, c_3) \quad (11c)$$

$$\theta_4 = \text{Atan2}(s_4, c_4) \quad (11d)$$

$$\theta_5 = -\theta_3 - \theta_4 \quad (11e)$$

$$\theta_6 = -\theta_2 \quad (11f)$$

$$v = \{(a_2 - y)c\alpha + (x - a_1)s\alpha\}l_{sz}s\theta_4 \quad (12)$$

$$w = l_{sz}^2(c_4^2 - 1) \{-2l_{tz}l_{sz}c_4 - xa_2s2\alpha - ya_1s2\alpha - 2xa_1c^2\alpha + y^2 + xys2\alpha + a_2^2 - l_{tz}^2 + a_1a_2s2\alpha + 2l_{fx}a_2s\alpha + l_{fx}^2 - 2ya_2 + x^2c^2\alpha + 2c\alpha a_1l_{fx} - l_{sz}^2 - 2l_{fx}ys\alpha - 2l_{fx}xc\alpha + 2ya_2c^2\alpha + a_1^2c^2\alpha - a_2^2c^2\alpha - y^2c^2\alpha\}, \quad (13)$$

$$s_3 = \sqrt{1 - c_3^2}, c_3 = \frac{p - \sqrt{q}}{l_{sz}^2 + 2l_{tz}l_{sz}c_4 + l_{tz}^4} \quad (14)$$

$$p = l_{tz}(x - a_1)c\alpha + l_{sz}(y - a_2)c_4s\alpha + l_{sz}(x - a_1)c_4c\alpha + l_{tz}(y - a_2)s\alpha - l_{tz}l_{fx} - l_{sz}l_{fx}c_4, \quad (15)$$